STUDY ON THRESHOLD EFFECT OF Mg-DOPED LITHIUM NIOBATE CRYSTALS*

FENG Xi-qi (冯锡淇), ZHANG Qi-ren (张启仁)**, YING Ji-feng (应继锋)
LIU Jian-cheng (刘建成) and YIN Zhi-wen (殷之文)
(*Shanghai Institute of Ceramics, Academia Sinica, Shanghai* 200050, *PRC*)

Received November 7, 1988.

Abstract

This paper presents measurements of OH^- absorption bands, fundamental optical absorption edge, lattice parameters, density, color center absorption spectra and Fe^{3+} ESR spectra at room temperature for a series of magnesium-doped and iron-doped lithium niobate crystals, and their dependence on magnesium concentration. It is observed that there exists the threshold effect of the magnesium dopant concentration in the measurements. The influence of the magnesium ion on the defect structure of magnesium-doped $LiNbO_3$ crystal is studied by use of the defect chemistry. The formation of various defect lattices in the crystal at different magnesium dopant concentrations, their growth and decay rules are proposed. Calculations indicate that the defect lattice with Nb-site Mg^{2+} will be formed in a congruent $LiNbO_3$ crystal when the MgO-doping level reaches 5.3%, which is taken as the main mark of the "threshold". The change caused by the "threshold" in the ionic environment of the $LiNbO_3$ crystal will serve to demonstrate the experimental results. And the calculation of the threshold concentration coincides with experiments. The conclusion in this paper can explain the reason for the drastic increase of anti-optical-damage capability in highly magnesium-doped $LiNbO_3$. This is significant for the research on the modification of other ABO_3-type electro-optic crystals.

Key words: Mg-doped $LiNbO_3$ crystals, threshold effect, defect chemistry.

I. Introduction

Of many ferroelectric crystals, lithium niobate has become a widely used electro-optic material. With the development of the technology of growing high-quality optical crystals, both the body and the waveguide of $LiNbO_3$ are applied to the laser technique, such as the electro-optic Q-swith, modulator, acoustic-optic filter and frequencydoubler. Recently, some new applications have been extended to the miniature CW and active internally Q-switched laser[1], the tunable subpicosecond infrared pulse generator[2], etc. However, the laser-induced refractive changes, namely the photorefractive effect, often seriously impede their applications in the field of laser. The photorefractive effect has been shown to be primarily due to the transition-metal ions, such as Fe and Cu present at the parts per million level in even the purest

* Project supported by the National Natural Science Foundation of China.
** Also in Suzhou Railway Normal College, Suzhou, PRC.

crystals[3,4]. Previous effects to smooth or resolve this problem were focused both on purification of starting material used in the crystal growth and on post-growth treatments, i.e. oxidation[5] and electrodiffusion[6], but little has been achieved.

Zhong et al.[7] reported that the resistance of $LiNbO_3$ to optical damage was greatly improved if more than 4.6% MgO was added to the congruent melt. Then Bryan[8], Sweeney and Halliburton[9] confirmed the result and observed the existence of the threshold effect with regard to Mg-doping levels, i.e. some properties, such as photoconductivity, the position of the OH^- absorption peak and the color center absorption spectra, would cause a sharp change when the Mg-doping level exceeded the threshold. They also discovered that the enhancement of the optical damage resistance was due to the increase by hundred times in the photoconductivity, rather than the decrease in the photovoltage current. Undoubtedly, the threshold effect marks a sharp change of the ionic environment from one type into another in the $LiNbO_3$ crystal. Sweeney et al. considered that there existed two types of Li-site Mg^{2+}, i.e. the simple Mg^+ ion $(Mg_{Li})^+$ and the Mg^+ complex[10]. Polgar et al. observed from measurements of the optical absorption edge and the conductivity that those magnesium ions exceeding the threshold concentration may yield some kinds of aggregates[11]. The analysis of photoconductivity by R. Gerson et al.[12] indicates that the enhancement of the photoconductivity of the heavy Mg-doped $LiNbO_3$ is attributed to a drastic reduction of the tapping cross section of Fe^{3+} for electrons. Accordingly, they proposed that the iron might substitute for Nb^{5+} rather than for Li^+. But in the aspect of crystal chemistry, such substitution might be complex. From the above assumptions arise three problems: (i) What is the physical essence of the Mg-doping level threshold effect? (ii) By what mechanism do the magnesium ions cause the sharp change of the ionic environment in $LiNbO_3$? (iii) Why can this sharp change greatly influence the behavior of the impurity ions, especially the transition-metal ions, in $LiNbO_3$?

This paper deals with the formation of defect lattices containing Mg^{2+} in the congruent crystal at different MgO-doping levels from the viewpoint of defect chemistry and proposes the concentration of the MgO-doping level threshold to be 5.3 mol%. The Mg^{2+} exceeding the threshold concentration will substitute Nb^{5+}. Systematic measurements of OH^- absorption spectra, optical absorption edge, lattice parameters, densities, color center absorption spectra and Fe^{3+} ESR spectrum for a group of congruent $LiNbO_3$:Mg (MgO: 1 mol%—9 mol% in melt) were performed, the MgO-doping level threshold effect was observed, and the experimental results were reasonably demonstrated by using the defect structure model.

II. Defect Chemistry of Mg-doped $LiNbO_3$ Crystals

The lithium niobate crystal is a typical non-stoichiometric compound. The congruent crystal grown with the Czochralski technique has a form of $(Li_2O)_{50-x}(Nb_2O_5)_{50+x}$, where x is the surplus Nb_2O_5 (mole), and $x = 1.4$. Each excessive Nb occupies an Li site, thus becoming Nb_{Li}, then leaves an Nb vacancy V_{Nb}[13] with its chemical equation

$$3Nb_2O_5 = 5[Nb_{Li}^{5+}(Nb_{Nb}^{5+})_{1/5}(V_{Nb})_{4/5}O_3^{2-}], \quad (1)$$

where $[Nb_{Li}^{5+}(Nb_{Nb}^{5+})_{1/5}(V_{Nb})_{4/5}O_3^{2-}]$ is a defect lattice with charge equilibrium, called

lattice [1]. The MgO doped in the crystal will collaborate with the excessive Nb_2O_5 and form a defect lattice:

$$Nb_2O_3 + MgO = 2[(Mg_{Li}^{2+})_{\frac{1}{2}}(V_{Li})_{\frac{1}{2}}Nb_{Nb}^{5+}O_3^{2-}], \quad (2)$$

called lattice [2]. As the MgO-doping amount increases to $2x$, lattice [1] disappears. The crystal contains only lattice [2] and the normal lattice $[Li_{Li}^{+}Nb_{Nb}^{5+}O_3^{2-}]$ while the MgO-doping level reaches 2.7 mol%. When the MgO-doping amount is larger than $2x$,

$$2[(Mg_{Li}^{2+})_{\frac{1}{2}}(V_{Li})_{\frac{1}{2}}Nb_{Nb}^{5+}O_3^{2-}] + MgO = 2[Mg_{Li}^{2+}Nb_{Nb}^{5+}O_3^{2-} + e^{-}] + O_i^0. \quad (3)$$

Let lattice [3] denotes $[Mg_{Li}^{2+}Nb_{Nb}^{5+}O_3^{2-}+e^{-}]$, where the magnesium on the Li-site Mg_{Li}^{2+} in +1-valence state traps one of the valence electrons from an O^{2-} and makes the electron a localized one, so that oxygen becomes an interstitial atom O_i^0. When the MgO-doping amount reaches $4x$, namely the MgO-doping level is 5.3 mol%, lattice [2] disappears and there is no more excessive Nb and V_{Li}. With the MgO-doping level increasing continuously, Mg^{2+} will occupy the Nb site and become Mg_{Nb}^{2+}, resulting in the formation of a new defect lattice [4]:

$$2[Mg_{Li}^{2+}Nb_{Nb}^{5+}O_3^{2-} + e^{-}] + 2MgO + O_i^0 = 3[Mg_{Li}^{2+}(Mg_{Nb}^{2+})_{\frac{1}{3}}(Nb_{Nb}^{5+})_{\frac{2}{3}}O_3^{2-}]. \quad (4)$$

Every three lattices [4] form a electroneutrality defect-lattice group as shown in Fig. 1, which contains three Mg_{Li}^{2+}, one Mg_{Nb}^{2+} and two Nb_{Nb}^{5+}. When MgO-doping amount reaches $8x$ and the MgO-doping level reaches 10.1 mol%, lattice [3] will disappear and there will be only perfect lattice and defect lattice [4].

When the MgO-doping level reaches 5.3 mol%, in the crystal there will be defect

Table 1

The Defective Lattice in the $LiNbO_3$ Crystals With Different MgO-doping Levels

Li/Nb	MgO-doping devel (mol%)	Defective Lattice[a)]
0.945	0	lattice [1]
0.945	0<MgO<2.7	lattice [1] + lattice [2]
0.945	2.7<MgO<5.3	lattice [2] + lattice [3]
0.945	5.3<MgO<10.1	lattice [3] + lattice [4]
0.945	MgO>10.1	lattice [4]

a) The normal lattice ($Li_{Li}^{+}Nb_{Nb}^{5+}O_3^{2-}$) has not been listed.

lattice [4], that is the origin of the "threshold effect" to be discussed later. Of course, the threshold concentration is related to the ratio Li/Nb of the grown crystal. Table 1 lists the defect-lattice types appearing in $LiNbO_3$ crystals at different MgO-doping levels.

The charge number, electronegativity and the ionic radius of Mg^{2+} and Nb^{5+} are +5, 1.7, 0.69 Å and +2, 1.2, 0.66 Å respectively, quite different from each other coordinately. Is it possible that Mg^{2+} occupies the Nb site? Smyth's study indicated that there existed such a great intrinsic ionic disorder in the $LiNbO_3$ crystal[14] as to tolerate the changes of the cation stacking sequences caused by Li-deficiency in composition. The Mg^{2+} occupying Nb site like Mg^{2+} occupying an Li site may come into another stable state by means of lattice relaxation. In fact, we can readily grow good-quality $LiNbO_3$:Mg crystals at an Mg^{2+}-doping level higher than the threshold concentration. This implies that it is not impossible for Mg^{2+} to occupy an Nb site.

III. Experimental Method

Superpure Nb_2O_5 and Li_2CO_3 were used as raw materials. All samples in this work are in congruent composition, Li/Nb = 0.945. MgO content in crystals under study are 0, 1.0, 2.7, 5.0, 6.0 and 9.0 mol% respectively. The Fe_2O_3 is used as the dopant, and the Fe-doped $LiNbO_3$ crystals obtained are Fe well-distributed. Owing to the high purity of materials, the automatic control technique and appropriate annealing and poling conditions, good-quality crystals without obvious growth streak were yielded. All the crystals used are listed in Table 1. Of them, the Mg content of crystals Nos. 2—5 was checked with a Philip PW1404 X-ray fluorescence spectrograph. The relative fluorescence intensity of the MgKα radiation of $LiNbO_3$:Mg crystals was found proportional to the MgO-doping level in the melt as shown in Fig. 2.

The infrared spectra were performed on a Nicolet 7000 infrared spectrometer. The

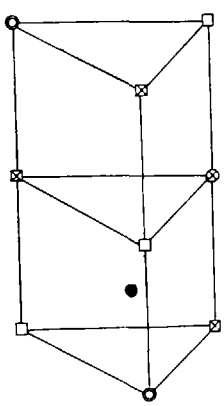

Fig. 1. Defect aggregation associated with 3-lattice [4], Mg_{Li}^{2+} $(Mg_{Nb}^{2+})_{2/3}O_3^{2-}$.
□, natural vacancy; ⊠, Mg_{Li}^{2+}; ◎, Nb^{5+}; ⊗, Mg_{Nb}^{2+}; ●, O^{2-}.

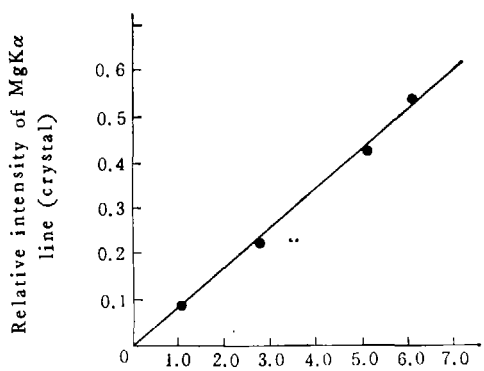

Fig. 2. Relation between the relative X-ray fluorescence intensity of MgKα line and the MgO-doping levels in $LiNbO_3$:Mg crystals.

Table 2

The $LiNbO_3$ Crystal Used in the Present Study

Sample No.	1	2	3	4	5	6	7	8
Li/Nb (melt)	0.945	0.945	0.945	0.945	0.945	0.945	0.945	0.945
MgO (melt, mol%)	0	1.0	2.7	5.0	6.0	9.0	6.0	0
Fe_2O_3 content[a] (crystal, ppm)	—	—	—	—	—	—	530	650

a) Fe_2O_3 contents were measured by atomic absorption spectrum. The Fe_2O_3 contents in sample Nos. 1—6 have not been measured.

wavenumber resolving power is better than 4 cm^{-1} (unpolarized light). The optical absorption edge and the color center absorption spectra were measured by a Beckman 5270 UV-VIS-Near IR spectrophotometer. The X-ray powder diffraction patterns of crystals Nos. 1—6 were taken by a D-500 diffractionmeter, using CuKα radiation. Accurate values of the lattice parameters a and c were obtained by the least-square analysis, ($2\theta = 85—105°$) is adjusted with an American SRM-640 pure silicon powder. The densities were measured with the Archimedes method on a balance of 0.2-mg sensitivity. The room temperature ESR measurement of the sample containing Fe^{3+} was performed on a Felex ESR spectrometer. The c-axis was parallel to the magnetic field with microwave frequency 9.129 GHz and modulation frequency 100 KHz.

IV. Experimental Results and Discussion

As shown above, Mg_{Nb}^{2+} is formed in the congruent $LiNbO_3$ crystal ($x=1.4$) when the Mg-doping level reaches 5.3 mol%, in company with lattice relaxation. It will cause the change in the ionic environment and a sharp change in the physical properties of the crystal, i.e. Mg-doping level threshold effect, as confirmed by the following experiments.

1. OH^- *Infrared Absorption Spectrum*

Fig. 3 shows the OH^- absorption spectra of samples Nos. 2—5. When the MgO-doping level $\leqslant 5.0$ mol%, no obvious changes of the peak position and the band shape were observed in the OH^- absorption spectrum that has a 3-peak structure. With the increase of the MgO-doping level, the small peak on the long-wavelength side rises slightly. When the MgO-doping level reaches 6.0 mol%, the OH^- absorption peak shifts towards the shorter-wavelength side, $\Delta\nu = 54$ cm^{-1}, the OH^- absorption band turns into a 2-peak structure, (H_1' and H_2'), with a sharper band. This indicates the change in the environment of the OH^- ions.

The H^+ ion in a $LiNbO_3$ crystal affected simultaneously by the polarization effect of the O^{2-} ion and the lattice positive ion behaves like an impurity ion weakly trapped by an O^{2-} ion, so the OH^- absorption spectrum is sensitive to the change of the ion environment. When the MgO-doping level exceeds the threshold concentration, Mg^{2+} may occupy the Nb site, forming a strongly negative-charge center $(Mg_{Nb})^{3-}$,

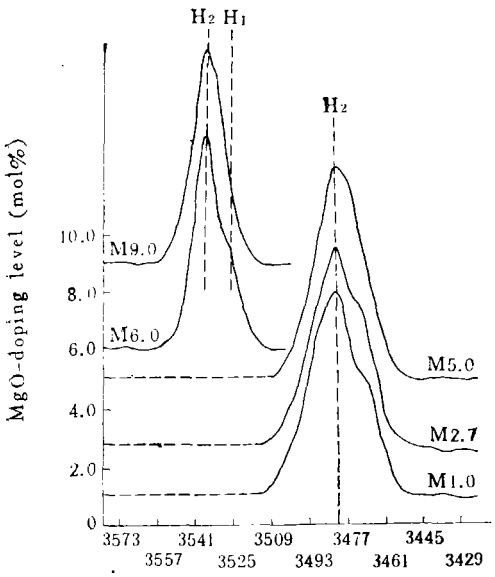

Fig. 3. OH^- infrared absorption bands of $LiNbO_3$:Mg crystals of various MgO-doping levels. (The spectra were measured at room temperature.)

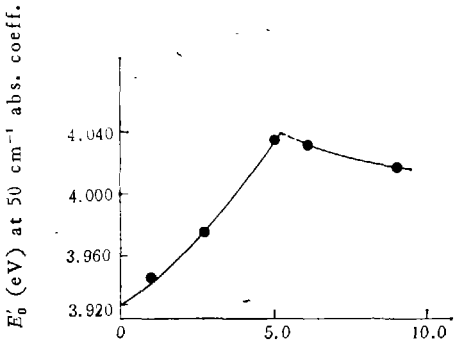

Fig. 4. Optical absorption edge as a function of the MgO-doping level in $LiNbO_3$:Mg crystals.

and H^+ tends to gather in its vicinity. The electronegativities of Mg^{2+} and Nb^{5+} are 1.2 and 1.7 respectively, the substitution of Mg^{2+} for Nb^{5+} will weaken the cation-oxygen bond of its neighbouring O^{2-} ion and strengthen the OH^- bond, resulting in the violet shift of the OH^- absorption band. This phenomenon is similar to the frequency shift of the OH^- absorption spectrum in the climoamphiboles mineral when Mg^{2+} substitutes Fe^{2+}[15].

2. *Optical Absorption Edge*

The shape of the optical absorption edge of the $LiNbO_3$ crystal is consistent with the Urbach rule:

$$A = A_0 \exp[\gamma(h\nu - E_0)],$$

where A is the optical absorption coefficient, $h\nu$ the photon energy, E_0 the cross-over point of extrapolated absorption edge and the photon energy coordinate axis, and γ is a constant related to the temperature. It is difficult to determine experimentally the exact position of the absorption edge of $LiNbO_3$. But what we are concerned about is the relative shift of the absorption edge. For the sake of simplicity, let the cross-over point E'_0 of the A-$h\nu$ curve and the photon energy coordinate (A=50 cm^{-1}) be the relative value E'_{g0} of the forbidden band width. It can be seen from Fig. 4 that the absorption edge keeps shifting toward the shorter-wavelength region with the increase of the MgO-doping level. This coincides with the fact that the absorption edge of the $LiNbO_3$ continuously shifts toward the shorter-wavelength region as the Li/Nb ratio increases from the congruent to stoichiometry. The modulation effect

of MgO on the absorption edge corresponds to the change of the Li/Nb ratio, and the Mg^{2+} dopant corresponds to the increase of the Li/Nb ratio. When the MgO-doping level reaches the threshold concentration, E'_{g0} would reaches its maximum as shown in Fig. 4. The E'_{g0} maximum occurs in the region between 5.0 and 6.0 mol% MgO-doping level. When the MgO-doping level exceeds the threshold concentration, Mg^{2+} may occupy the Nb site that the lattice relaxation makes a deformation region, different from a normal lattice. We have pointed out that the orderly distribution of the high-concentration point defects in a nonstoichiometric crystal has the modulation effect on the gap of the forbidden band, and the interaction of the potential field of the lattice deformation region causes the energy gap-contraction and the redshift of the optical absorption edge[16]. Therefore, a possible explanation to the experimental result shown in Fig. 4 is that the above-mentioned lattice-deformed region will be stable with minimum energy only when the high-concentration point defects are orderly distributed. Its modulation effect on the energy gap is similar to the lattice relaxation region caused by the occupation of the Li site by Nb when the MgO-doping level is below the threshold concentration, all causing energy gap-contraction, which results in the redshift of the optical absorption edge. The redshift varies with the degree of the lattice deformation.

3. *Measurements of Lattice Parameters and Density*

X-ray diffraction measurements indicated that all the crystals used in this study were single-domain crystals without phase separation or phase transition.

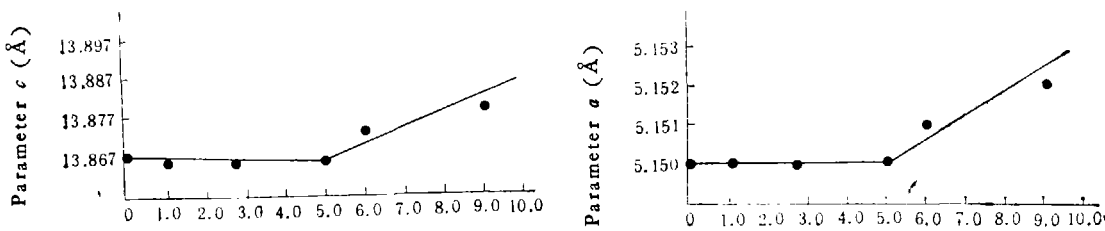

Fig. 5. Relation between the lattice parameters of $LiNbO_3$:Mg crystals and the MgO-doping levels.

(a) Lattice parameter c; (b) lattice parameter a.

Fig. 5 shows the measurement results of the lattice parameters a and c, and Fig. 6 presents the calculated and measured X-ray densities of a group of samples. It can be seen from Fig. 5 that when MgO-doping level is lower than or equal to 5 mol%, the lattice parameters a and c keep substantially unchanged. When the MgO-doping level exceeds 6.0 mol%, the lattice parameters increase. It can be seen from Fig. 6 that the tendency to the change of the calculated density with the increasing of the MgO-doping level is in good agreement with that of the measured density. As the MgO-doping level exceeds the threshold concentration, the density decreases obviously.

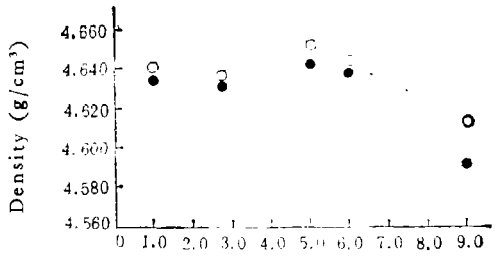

Fig. 6. Comparison between the measured density data of $LiNbO_3$ and the X-ray density data obtained from the suggested model.

○, X-ray density; ●, measured density.

The charge number and the electronegativity of Mg^{2+} and Nb^{5+} are +2, +5 and 1.2, 1.7 respectively. Therefore the Mg—O bond is weaker than the Nb—O bond. When an Mg^{2+} ion substitutes an Nb^{5+} ion, its neighbor O^{2-} ions will relax outward, so that the volume oxygen octahedron surrounding Mg^{2+} becomes bigger than that of the oxygen octahedron surrounding Nb^{5+}, and the lattice parameters increase while the density decreases.

4. *Color Center Absorption Spectra*

Fig. 7 shows the optical absorption curves of samples Nos. 1—5 which were annealed in vacuum. Meanwhile, this figure manifests that the absorption spectra of the crystals with MgO-doping level ≤5 mol% are in accordance with that of the undoped crystal, expressed by a broad band (curve 1) 300—800 nm wide, and its peak positioned at 2.6 eV (~500 nm). When the MgO-doping level reaches 6.0 mol%, the color center absorption band shifts to the near infrared region, and the peak position shifts to 0.85 eV (1460 nm) accompanied by a small peak identified with an absorption band caused by F^+-center, at 1.6 eV (780 nm)[9]. The color center absorption band corresponds to the $1s \rightarrow 2p$ transition of the F-center, and its peak position

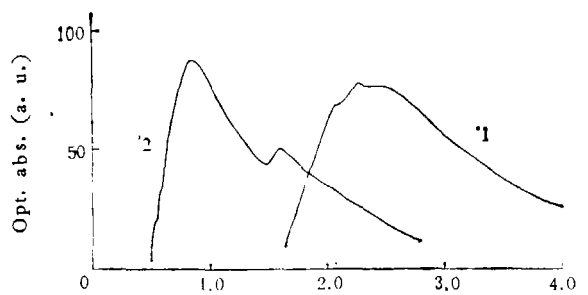

Fig. 7. Optical absorption from reduced $LiNbO_3$:Mg crystal (vacuum anneal at 1000℃ for 0.5 h).

1, Taken from $LiNbO_3$:Mg crystals with MgO-doping levels 5 mol%;

2, taekn from a 6 mol% MgO $LiNbO_3$ crystal.

1, MgO≤5 mol% reduced; 2, MgO = 6 mol% reduced.

and the band shape are related with the property and symmetry of the coordination. The F-center in undoped $LiNbO_3$ has six nearest neighbouring sites occupied separately by two Nb^{5+}, two Li^+ and two vacant sites, which form a triangle pillar coordinate. Since the Nb–O bond has a rather strong covalent property, an (F^+, Nb^{4+})-associated color center is formed[17]. In an $LiNbO_3$:Mg crystal with a low Mg concentration, an (F^+, Nb^{4+})-associated color center disturbed by an $(Mg_{Li})^{+1}-(V_{Li})^{-1}$ dipole is formed, and both centers share the same absorption spectrum. In a crystal with an Mg concentration higher than the threshold, an F-center near an Mg^{2+}_{Nb} has four nearest neighboring sites occupied by two Mg^{2+}_{Nb} and one Nb^{5+}_{Nb} separately and forms a $\left[\begin{matrix}Mg\\Nb\end{matrix}\right\rangle F \left\langle\begin{matrix}Mg\\Nb\end{matrix}\right]$-associated color center. Strongly influenced by the $(Mg_{Nb})^{3-}$ negative center, the F-center's electronic cloud expands outward, so that its 1*s*-state rises and the $1s \rightarrow 2p$ transition energy drops, resulting in a large redshift of the color center absorption band. The defect structure and the color center absorption spectra of the $LiNbO_3$:Mg crystal will be dealt with elsewhere.

5. *ESR Spectrum of* Fe^{3+}

Fig. 8 shows the room-temperature ESR spectra of the $LiNbO_3$:(Mg + Fe) (sample No. 7) and the $LiNbO_3$: Fe (sample No. 8) (experiment reported in Ref. [9] was fulfilled under 77 K). It can be seen from Fig. 8 that there exists obvious difference not only in the ESR spectra, but also in the OH^- absorption spectra of these two samples, which indicates that Fe^{3+} occupies different lattice sites in two samples[8]. In a congruent $LiNbO_3$:Fe crystal, Fe^{3+} occupies an Li site [17], and when the MgO-doping level exceeds the threshold concentration, the Fe^{3+} may enter the lattice in two possible ways: (i) it is easier for Fe^{3+} than for Mg^{2+} to occupy an Nb^{5+} site according to the charge number and electronegativity; (ii) Fe^{3+} may occupy an Nb site and an Li site in pairs and keep charge equilibrium. From Fig. 8 it can be seen that the Fe^{3+} ESR signal occurs in $LiNbO_3$:Fe, but disappears in $LiNbO_3$:(Mg + Fe) crystal (sample No. 7). This implies that in this crystal Fe^{3+} occupies

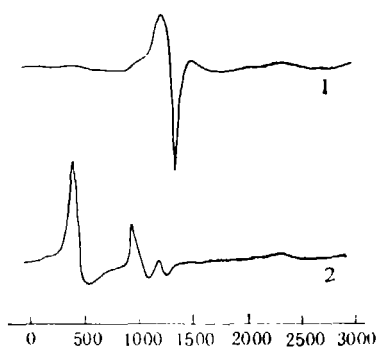

Fig. 8. ESR spectrum taken at room temperature, H//C axis.
1, (6 mol% MgO + 530 ppm Fe)-doped $LiNbO_3$ (No. 7); 2, 650 ppm Fe-doped $LiNbO_3$ (No. 5).
1, $LiNbO_3$:Mg:Fe; 2, $LiNbO_3$:Fe.

merely one type of lattice site, i.e. Fe_{Nb}, accompanied by lattice relaxation.

The photorefractive effect depends primarily on the impurity of some transition-metal in the crystal. Taking Fe as an example, the main electronic process of the photorefractive effect is

$$Fe^{2+} \longrightarrow Fe^{3+} + \text{Photoelectron } (Fe^{2+} \text{ ionization}),$$

$$Fe^{3+} + \text{Electron} \longrightarrow Fe^{2+} + \text{Phonon } (Fe^{3+} \text{ trapping an electron}),$$

where the most important process parameter is the cross section of Fe^{3+} for electron capture. The Li-site $Fe^{3+}(Fe^{3+}_{Li})$ displays locally +2 valance , and the Nb-site Fe^{3+} (Fe^{3+}_{Nb}) still displays electric negativity even with the lattice relaxation taken into consideration and a smaller cross section for electron capture than Fe^{3+}_{Li}. This may be the main reason for the enhancement by hundreds of times of the photoconductivity of the heavy Mg-doped $LiNbO_3$ crystal. It can be expected that the change of the site occupation by Fe^{3+} will influence the excitation process of the photoelectron, as well as the response rate of the photorefractive effect.

V. Conclusion

The experimental results of the above congruent $LiNbO_3$ crystals with the MgO-doping level being 0, 1.0, 2.7, 5.0, 6.0 and 9.0 mol% respectively indicate the existence of a so-called Mg-doping level concentration threshold effect. Various properties of the crystal will change drastically when the MgO-doping level exceeds the threshold concentration. The OH^- absorption band shifts toward the violet side and will grows narrower. The optical absorption edge shifts toward the longer wavelength side after passing the maximum. The lattice paramaters a, c and the measured density change significantly. The color center absorption spectrum shifts to the nearinfrared region and the room temperature Fe^{3+} ESR signal shifts to the higher magnetic field. The Mg-doping level threshold concentration indicated by experiments ranges in 5.0—6.0 mol% MgO.

It can be concluded from the discussion of the defect structure in $LiNbO_3$:Mg crystals that (i) there are different types of Mg-contained defect lattices in the crystals at different Mg-doping levels, (ii) the threshold concentration is 5.3 mol% MgO in congruent crystals, which coincides with the experimental results and (iii) when the Mg-doping level exceeds the threshold, there will be Nb-site Mg^{2+} (Mg^{2+}_{Nb}) which is the main source causing a sharp change of the ionic environments in the crystal. These conclusions are used to explain the experimental results in this paper.

Mg^{2+} differs greatly from Nb^{5+} in charge numbers, electronegativity and ionic radius, which makes it difficult to occupy the Nb site. But the intrinsic structure characteristics of the $LiNbO_3$ crystal makes the site occupation possible. What should be further studied is what kind of stable local structure caused by the lattice relaxation will be formed near Mg_{Nb}.

Yet, the experimental results in this paper provide only indirect evidence for Mg^{2+} occupying the Nb site. We are performing high-resolution NMR measurements

in an expectation to get direct evidences.

That some transition-metal ions, such as Fe, occupy the Nb site instead of Li site in $LiNbO_3$, caused by the Mg-doping level threshold effect, may be the main reason of the fact that the optical-damage resistance has been enhanced by hundreds of times in heavy Mg-doped $LiNbO_3$ crystal. This conclusion can also be principally suitable to the modification of other ABO_3 electro-optic crystals: LiTaO, $KNbO_3$, etc.

The authors thank Wang Jin-chang, Ma Yi-xian, Zhu Quan-bao and Wu Yao-an, for providing the crystals used in the study.

References

[1] Moore, D. S. & Schmidt, S. C., *IEEE. J. Quan. Electron*, **23**(1987), 262.
[2] Amado Cordeva-Plaza et al., *Opt. Lett.*, **12**(1987), 480.
[3] Glass, A. M., *Opt. Eng.*, **17**(1978), 470.
[4] Peterson, G. E. et al., *Appl. Phys. Lett.*, **19**(1974), 130.
[5] Jorgensen, P. J. & Barlett, R. W., *J. Phys. Chem. Solids*, **30**(1969), 2639.
[6] Smith, R. G. et al., *J. Appl. Phys.*, **30**(1968), 4600.
[7] Zhong Gi-guo et al., *11th Inter. Quan. Electro. Con.*, *IEEE Con.*, No. 80 CH 15610-0, June, 1980, 631.
[8] Bryan, D. A. et al., *Appl. Phys. Lett.*, **44**(1984), 847.
[9] Sweeney K. L. et al., *ibid.*, **45**(1984), 805.
[10] ————, *J. Appl. Phys.*, **57**(1985), 1036.
[11] Polgar. K. et al., *Sol. Commun.*, **59**(1986), 375.
[12] Gerson, R. et al,, *J. Appl. Phys.*, **60**(1986), 3553.
[13] Abrahams, S. C. & Marsh, P., *Acta Cryst.* **B-42**(1986), 61.
[14] Smyth, D. M., *Ferroelectrics*, **50**(1983), 50.
[15] Burns, R. G., *Science*, **513**(1966), 890.
[16] Feng Xiqi et al., in *Proc. of 6th Inter. Symp. on Appl. of Ferroelectrics*, Leihigh University, USA, June 1986, 29.
[17] 冯锡淇等，中国科学A辑，1987，6：614.
[18] 冯锡淇等，科学通报，**33**(1988)，13:1001.